Available online at www.sciencedirect.com

SciVerse ScienceDirect

Ceramics International 39 (2013) 4363–4367

CERAMICS INTERNATIONAL

www.elsevier.com/locate/ceramint

Characterization and electrochemical performance of $(Ba_{0.6}Sr_{0.4})_{1-x}La_xCo_{0.85}Ti_{0.15}O_3$ as cathode materials for intermediate temperature solid oxide fuel cell

Yongna Shen[a], Hailei Zhao[a,b,*], Deqiang Teng[a], Zhihong Du[a]

[a]School of Materials Science and Engineering, University of Science and Technology Beijing, Beijing 100083, China
[b]Beijing Key Laboratory of New Energy Materials and Technology, Beijing 100083, China

Received 8 October 2012; received in revised form 10 October 2012; accepted 7 November 2012
Available online 14 November 2012

Abstract

Cubic perovskite-type $(Ba_{0.6}Sr_{0.4})_{1-x}La_xCo_{0.85}Ti_{0.15}O_{3-\delta}$ (BSLCT, $0 < x < 0.2$) materials were synthesized and evaluated as cathode for intermediate temperature solid oxide fuel cell (IT-SOFC) based on $Ce_{0.9}Gd_{0.1}O_{2-\delta}$ (GDC). The influence of La-doping on the lattice structure, electrical conductivity, chemical compatibility with electrolyte GDC, and cathode performance of BSLCTs were studied. The solid solution limit of La in BSLCT was ca. $x=0.15$. These materials displayed small polaron hopping conduction behavior. With increasing La content, the electrical conductivity increased, mainly due to the decreased activation energy for hopping conduction. BSLCT had a good compatibility with GDC at temperatures below 900 °C, above which, a slight diffusion was observed. La doping had a positive effect on the cathode performance of BSLCT. A maximum power density of 255 mW cm^{-2} was obtained when La content was $x=0.15$ for BSLCT/GDC (300 μm)/Ni–GDC cell.

Keywords: B. Defects; C. Electrical conductivity; E. Electrodes; E. Fuel cells

1. Introduction

Nowadays, considerable studies have been carried out on the development of intermediate temperature solid oxide fuel cells (IT-SOFCs). From a materials point of view, lowering the operating temperature of SOFC to an intermediate range could increase the durability of key cell components both thermally and mechanically, as well as enable the use of cheaper metallic materials for interconnect/current collectors [1,2]. However, on the other hand, it also makes traditional cathode based on $La_{1-x}Sr_xMnO_{3-\delta}$ (LSM) materials suffer from a large polarization loss at this temperature range [3,4]. With the aim of reducing polarization loss, mixed ionic–electronic conductors, Co-based mixed ionic–electronic conductors, such as $La_{1-x}Sr_xCoO_3$ (LSC) and $La_{1-x}Sr_xFe_{1-y}Co_yO_3$ (LSFC), have been investigated and are considered as attractive alternative cathode materials due to their extended oxygen reduction active sites from three phase boundary to the entire cathode surface and good catalytic activity [5–9]. Recently, $Ba_{0.5}Sr_{0.5}Co_{0.8}Fe_{0.2}O_3$ (BSCF) was reported to have an even lower polarization loss, the area-specific resistance of which was only 0.055–0.071 Ω cm^2 at 600 °C and 0.156–0.61 Ω cm^2 at 500 °C [10]. With it as cathode, an anode-support cell can reach a peak power density of 1010 mW cm^{-2} at 600 °C. Although BSCF has excellent electrochemical performance, its high temperature expansion coefficient (TEC) ($19-24\times10^{-6}$ K^{-1}) [11,12] causes matching problem with other cell components and limits its practical applications. As is known, the high TEC of BSCF is mainly attributed to the formation of vacancies due to the reduction of Fe^{4+} and Co^{4+} to lower valence state [11,13]. To overcome the issue of thermal expansion, in our previous work, the more chemical stably Ti ion was introduced into the Co site forming $Ba_{0.6}Sr_{0.4}Co_yTi_{1-y}O_3$

*Corresponding author at: University of Science and Technology Beijing, School of Materials Science and Engineering, 30 Xueyuan Road, Haidian District, Beijing 100083, China. Tel./fax: +86 10 82376837.
E-mail address: hlzhao@ustb.edu.cn (H. Zhao).

0272-8842/$ - see front matter © 2012 Elsevier Ltd and Techna Group S.r.l. All rights reserved.
http://dx.doi.org/10.1016/j.ceramint.2012.11.022

(BSCT) and the TEC was reduced to $\sim 14 \times 10^{-6}\,K^{-1}$ [14]. However, Ti-doping resulted in a negative effect on electrical conductivity and thus decreasing the cathode performance.

Considering that materials containing rare earth such as $La_{1-x}Sr_xFe_{1-y}Co_yO_3$ and $Sm_{1-x}Sr_xCoO_3$ always exhibit high electrical conductivity [8,15,16], in present work, La was selected as donor dopant on A site of BSCT to enhance the electrical conductivity and improve the electrochemical properties. The effect of La doping on the crystal structure and the electrical conductivity of $(Ba_{0.6}Sr_{0.4})_{1-x}La_xCo_{0.85}Ti_{0.15}O_{3-\delta}$ (BSLCT) materials was investigated. The chemical compatibility with electrolyte GDC and the cathode performance on GDC electrolyte supported cells were evaluated.

2. Experimental

2.1. Material and cell preparation

A series of $(Ba_{0.6}Sr_{0.4})_{1-x}La_xCo_{0.85}Ti_{0.15}O_{3-\delta}$ $(0 < x \leq 0.2)$ powders were prepared by the solid state reaction method. Stoichiometric mixtures of the starting materials $BaCO_3$, $SrCO_3$, La_2O_3, TiO_2 and $C_4H_6CoO_4 \cdot 4H_2O$ were ball milled in ethanol for 5 h. After drying, the mixtures were ground using agate mortar and passed through a 150-mesh sieve. The obtained fine green powders were calcined at 900 °C for 10 h with a heating and cooling rate of 3 °C min^{-1}. Afterwards, the calcined powders were uniaxially pressed into bars (40 mm × 7 mm × 3 mm) at a pressure of 150 MPa and then sintered at 1100 °C for 10 h to get dense samples for bulk density and electrical conductivity testing.

The single-cells with GDC as electrolyte were fabricated using the screen-printing method. Dense electrolyte pellets, about 12 mm diameter, were obtained by pressing GDC powders under ca. 115 MPa uniaxial force, followed by sintering at 1500 °C in air for 6 h. The pellets were then polished with no. 600 grit paper to 300 μm in thickness and then cleaned with ethanol solution. The anode inks prepared by mixing Ni–GDC (60:40 wt%) composite with terpineol consisting of 10 wt% ethylic cellulose in a mass ratio of 6:4 using agate mortar were screen painted on the side of GDC electrolyte and fired at 1300 °C for 2 h. The BSLCT cathode inks obtained with the same method as anode were screen printed on the other side of GDC pellets with an active electrode area of 0.5 cm^2 and then fired at 900 °C for 2 h to form a porous cathode adhered well with electrolyte. After that, Pt paste was used as current collection while Ag wires as lead wire for both electrodes and fired at 800 °C for 0.5 h.

2.2. Characterization

The crystal structure and phase composition of synthesized powders were identified with X-ray diffraction (XRD, Rigaku D/max-A Diffractometer) using Cu $K_\alpha 1$ radiation. The relative densities of all sintered bars were measured by Archimedes' method with distilled water as the intrusion medium. All the samples had a density of higher than 90% of the theoretical density. Electrical conductivity measurements were performed by the four-terminal method [14] in the temperature range of 300 to 900 °C in static air. All the data were collected at equilibrate state after holding at each temperature for at least 15 min when no significant change in voltage and current were observed.

In order to check chemical compatibility of BSLCT with GDC electrolyte, powders of BSLCT and GDC were mixed in a 1:1 weight ratio and pressed into pellet before being fired at desired temperature for 5 h. Then the pellet was crushed into powder and analyzed by XRD to identify the phases.

Fuel-cell performances were tested using an in-house built test station. The single cell was sealed on an alumina tube with a glass ring as sealant. Humidified hydrogen (3% H_2O) with a flow rate of 50 ml min^{-1} was fed into the anode side as fuel, while only static air was used as oxidant in cathode side. The current–voltage (I–V) curve was obtained by monitoring the current and the terminal voltage under various loads at fixed temperature.

3. Result and discussion

The XRD patterns of the calcined BSLCT powders are shown in Fig. 1(a). All the samples presented a single cubic perovskite structure except the one with $x=0.2$, where some additional peaks indexed as $BaCoO_2$ were detected. This suggests that the limit of La doping in this series of BSLCT materials should not be more than 20 mol%. With increasing La content, the diffraction peaks of BSLCT shifted slightly to high-angle direction, as can be seen clearly from Fig. 1(b), indicating the shrinkage of crystal parameters. Doping the Ba/Sr site with La, on one hand, may decrease the cell parameter due to the smaller radii of La^{3+} ($r_{La^{3+}} = 1.36$Å) compare with that of Ba^{2+} ($r_{Ba^{2+}} = 1.61$Å) and Sr^{2+} ($r_{Sr^{2+}} = 1.44$Å). On the other hand, it can also result in the reduction of Co ions from Co^{4+} ($r_{Co^{4+}}$(high spin)$=0.53$ Å) to lower valence state Co^{3+} ($r_{Co^{3+}}$(high spin)$=0.61$ Å) [17] as charge compensation, thereby, increasing the cell parameter. In view of the changes in the cation radius of A and B sites, the size of La ion had a stronger effect on the cell parameter than its valence state. In addition, there was a loss of intensity of XRD peaks with La-doping level, indicating that the substitution of La decreased the crystallinity of the cubic structure of BSLCT.

The temperature dependence of total electrical conductivity of BSLCF with La-doping level is shown in Fig. 2(a). Since the ionic conductivity is always at least one order of magnitude lower than the electronic conductivity in perovskite mixed conductors [18,19], the measured total electrical conductivity can be regarded as the electronic conductivity. With increasing temperature, the electrical conductivities displayed an increase tendency though a

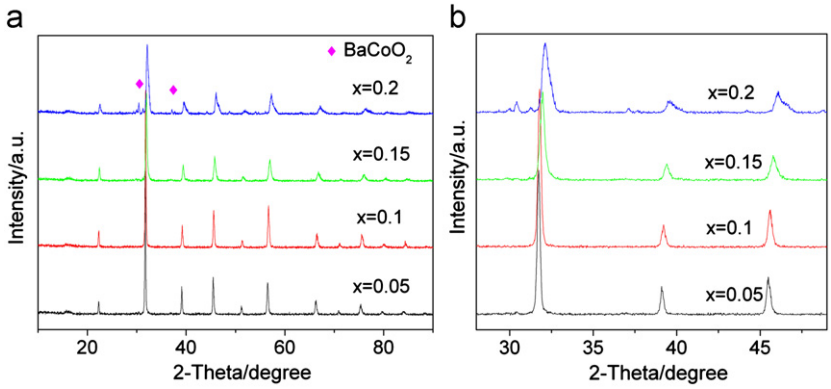

Fig. 1. XRD patterns of $(Ba_{0.6}Sr_{0.4})_{1-x}La_xCo_{0.85}Ti_{0.15}O_{3-\delta}$ sintered at 1100 °C in air for 10 h: (a) $10° \le 2\theta \le 90°$ and (b) magnified patterns with $28° \le 2\theta \le 49°$.

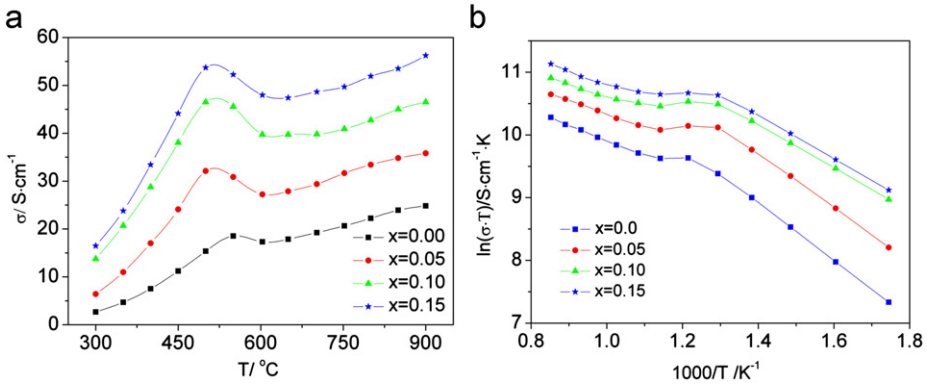

Fig. 2. Temperature dependence of the electrical conductivity of $(Ba_{0.6}Sr_{0.4})_{1-x}La_xCo_{0.85}Ti_{0.15}O_{3-\delta}$ ($x=0-0.15$) ceramics sintered at 1100 °C.

Table 1
Calculated activation energy for electronic hole hopping in $(Ba_{0.6}Sr_{0.4})_{1-x}La_xCo_{0.85}Ti_{0.15}O_{3-\delta}$ materials ($0 \le x \le 0.15$).

BSLCT/mol	E_a/eV	
	Low temp. range (300–500 °C)	High temp. range (600–900 °C)
$x=0.00$	0.393 ± 0.003	0.202 ± 0.008
$x=0.05$	0.365 ± 0.005	0.176 ± 0.006
$x=0.10$	0.291 ± 0.004	0.136 ± 0.009
$x=0.15$	0.289 ± 0.004	0.135 ± 0.011

temporary decrease was observed in the temperature range of 500–600 °C. As this abnormity corresponds to the negative deviation from linear relationship in their Arrhenius plots (Fig. 2(b)), the decrease of electrical conductivity is attributed to the release of lattice oxygen [20,21], which will result in partial annihilation of charge carrier concentration (electron holes), as expressed by

$$O_O^{\times} + 2h^{\bullet} \rightarrow V_O^{\bullet\bullet} + \frac{1}{2}O_2(g) \quad (1)$$

At a given temperature, the electrical conductivity increased steadily with increasing La content. The obvious increase in conductivity by La-doping can be considered from two factors, charge concentration (C) and activation energy (E_a) for charge transport. From the viewpoint of defect chemistry, La-doping will cause the reduction of Co ions from Co^{4+} to Co^{3+} in order to maintain the electrostatic neutrality of materials. As a result, the charge concentration (electronic hole) is reduced, as expressed by Eq. (2), which should lead to the decrease in electrical conductivity.

$$La_2O_3 + 2Co_{Co}^{\bullet} \xrightarrow{Ba_{0.6}Sr_{0.4}Co_{0.85}Ti_{0.15}O_3} 2La_{(Ba/Sr)}^{\bullet} + 2Co_{Co}^{\times} + 3O_O^{\times} \quad (2)$$

On the other hand, La-doping also makes change on the activation energy of electrical conduction. As shown in Fig. 2(b), the Arrhenius plots showed nearly linear feature in the temperature range of below 500 °C and above 600 °C, suggesting that the small polaron hopping was the predominant mechanism for the electrical conduction in these two

temperature ranges. The E_a can be derived by the slope of the fitted lines in Arrhenius plot according to

$$\sigma = \left(\frac{A}{T}\right)\exp\left(\frac{-E_a}{kT}\right) \quad (3)$$

where A is the materials constant containing the carrier concentration term, E_a is the activation energy for hopping conduction. The calculated E_a values for different samples in two temperature ranges are listed in Table 1. They decrease with increasing La-doping level in both temperature ranges, suggesting that La-doping facilitates the electronic hole hopping process in BSLCT materials. Compared to the charge concentration, the activation energy E_a for electron conduction plays more important role in the conductivity change of BSLCT.

The XRD patterns of BSLCT–GDC mixture in 1:1 weight ratio after heat treatment at different temperatures are shown in Fig. 3. It was clear that after calcination at 800 °C for 5 h, both compounds still retained their own structures. On increasing the calcination temperature up to 900 °C, although no new identifiable peaks were observed, there was a dramatic broadening in the intensity peaks at $2\theta = 45.5$ and 56°, indicating that there was a reaction and/or inter-diffusion of elements between BSLCT cathode and GDC electrolyte.

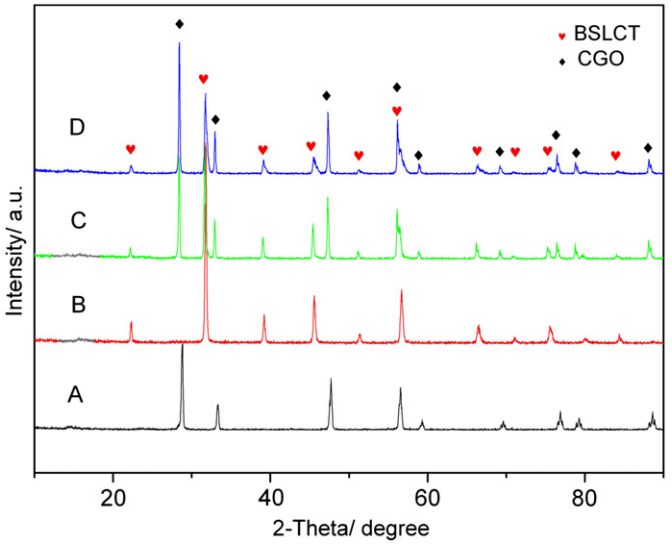

Fig. 3. XRD patterns of $(Ba_{0.6}Sr_{0.4})_{0.85}La_{0.15}Co_{0.85}Ti_{0.15}O_{3-\delta}$ BSLCT–GDC mixed powders sintered at different temperatures for 5 h, (A) GDC; (B) BSLCT; (C) BSLCT–GDC sintering at 800 °C; (D) BSLCT–GDC sintering at 900 °C.

Fig. 4 displays the cell voltage and power density as a function of current density for the cells BSLCT/GDC/Ni–GDC. All the cell voltages linearly decreased with increasing temperature, demonstrating that there was no polarization loss in the cells. As depicted in Fig. 4(a), the maximum power density of BSLCT ($x=0.15$)/GDC/Ni–GDC cell increased with temperature, due to the decrease in internal resistance of the cell where the greatest contribution was from electrolyte. With increasing La content in BSLCT, the power density increased steadily, which was considered to be mainly caused by the high electrical conductivity when more La was added to the A site. The maximum power density of ~255 mW cm^{-2} was obtained for the samples with $x=0.15$ at 800 °C. After optimization on the electrolyte thickness and the cathode microstructure, it is believed that the performance of the BSLCT-based cell could be further improved.

4. Conclusions

A series of cubic perovskite-type $(Ba_{0.6}Sr_{0.4})_{1-x}La_xCo_{0.85}Ti_{0.15}O_{3-\delta}$ $(0 < x \leq 0.2)$ materials were synthesized and the influence of La doping on the lattice structure and electrical properties was studied in relation to their potential use as cathode materials for SOFC. The solid solution limit of La in BSLCT is ca. $x=0.15$ at 1100 °C. The lattice parameter of BSLCT materials decreases with La-doping level. BSLCT has a good chemical compatibility with GDC electrolyte at temperature below 900 °C, a reaction and/or solid solution between the two com-;ponents may occur at temperature higher than 900 °C. With increasing temperature, the electrical conductivity increases steadily but showing temporary decrease in the temperature range of 550–600 °C. La doping increases the electrical conductivity remarkably, owing to the decreased activation energy for hopping conduction. Substitution of La in BSLCT improves the cathode performance obviously. For the cells BSLCT/GDC/Ni–GDC, the

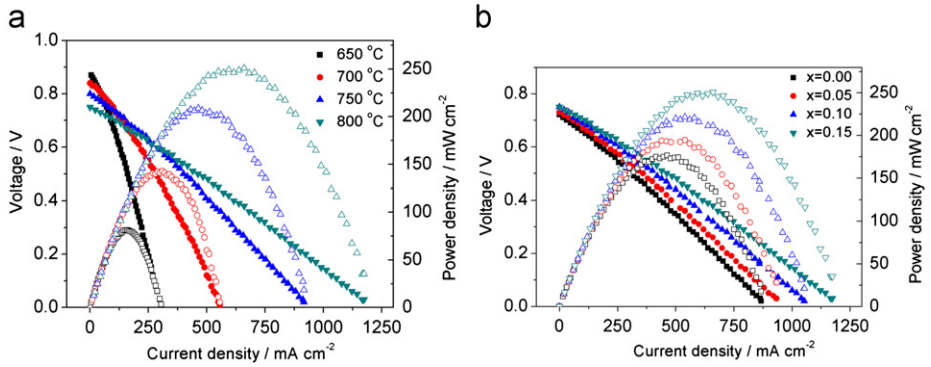

Fig. 4. Performance of the electrolyte-supported BSLCT/GDC/Ni–GDC half cells with 300 μm-thickness GDC electrolyte: I–V and I–P curves for BSLCT with $x=0.15$ at different temperatures (a) and for BSLCT with different La contents at 800 °C (b).

maximum power density is $\sim 255\ \mathrm{mW\ cm^{-2}}$ when $x=0.15$ at 800 °C. Considering that the electrolyte is relatively thick (300 μm) and the total conductivity of the GDC we prepared is much lower ($6.0\times10^{-3}\ \mathrm{S\ cm^{-1}}$ at 600 °C) than that reported ($>1.0\times10^{-2}\ \mathrm{S\ cm^{-1}}$) [22,23], the cell performance is encouraging. One would expect higher power densities using a thin-film electrolyte.

Acknowledgments

The authors gratefully acknowledge financial support from National Nature Science Foundation of China (No. 20973021), Nature Science Foundation of Beijing (No. 2102031) and Outstanding Doctoral Dissertation Guidance Foundation of Beijing (YB20091000802).

References

[1] Q. Liu, K. Khor, S. Chan, High-performance low-temperature solid oxide fuel cell with novel BSCF cathode, Journal of Power Sources 161 (2006) 123–128.
[2] J.W. Fergus, Metallic interconnects for solid oxide fuel cells, Materials Science and Engineering A 397 (2005) 271–283.
[3] J. Richter, P. Holtappels, T. Graule, T. Nakamura, L.J. Gauckler, Materials design for perovskite SOFC cathodes, Monatshefte Fur Chemie 140 (2009) 985–999.
[4] S.P. Jiang, Development of lanthanum strontium manganite perovskite cathode materials of solid oxide fuel cells: a review, Journal of Materials Science 43 (2008) 6799–6833.
[5] C. Sun, R. Hui, J. Roller, Cathode materials for solid oxide fuel cells: a review, Journal of Solid State Electrochemistry 14 (2009) 1125–1144.
[6] F. Tietz, V. Haanappel, A. Mai, J. Mertens, D. Stover, Performance of LSCF cathodes in cell tests, Journal of Power Sources 156 (2006) 20–22.
[7] M. Katsuki, S. Wang, M. Dokiya, T. Hashimoto, High temperature properties of $La_{0.6}Sr_{0.4}Co_{0.8}Fe_{0.2}O_{3-\delta}$ oxygen non-stoichiometry and chemical diffusion constant, Solid State Ionics 156 (2003) 453–461.
[8] A. Petric, P. Huang, F. Tietz, Evaluation of La–Sr–Co–Fe–O perovskites for solid oxide fuel cells and gas separation membranes, Solid State Ionics 135 (2000) 719–725.
[9] Y. Teraoka, T. Nobunaga, K. Okamoto, N. Miura, N. Yamazoe, Influence of constituent metal cations in substituted $LaCoO_3$ on mixed conductivity and oxygen permeability, Solid State Ionics 48 (1991) 207–212.
[10] Z. Shao, S.M. Haile, A high-performance cathode for the next generation of solid-oxide fuel cells, Nature 431 (2004) 170–173.
[11] Q. Zhu, T. Jin, Y. Wang, Thermal expansion behavior and chemical compatibility of $Ga_xSr_{1-x}Co_{1-y}Fe_yO_{3-\delta}$ with 8YSZ and 20GDC, Solid State Ionics 177 (2006) 1199–1204.
[12] J.F. Vente, S. McIntosh, W.G. Haije, H.J.M. Bouwmeester, Properties and performance of $Ba_xSr_{1-x}Co_{0.8}Fe_{0.2}O_{3-\delta}$ materials for oxygen transport membranes, Journal of Solid State Electrochemistry 10 (2006) 581–588.
[13] A. Manthiram, J.H. Kim, Y.N. Kim, K.T. Lee, Crystal chemistry and properties of mixed ionic–electronic conductors, Journal of Electroceramics (2011) 1–15.
[14] H. Zhao, D. Teng, X. Zhang, C. Zhang, X. Li, Structural and electrochemical studies of $Ba_{0.6}Sr_{0.4}Co_{1-y}Ti_yO_{3-\delta}$ as a new cathode material for IT-SOFCs, Journal of Power Sources 186 (2009) 305–310.
[15] T. Ishihara, M. Honda, T. Shibayama, H. Minami, H. Nishiguchi, Y. Takita, Intermediate temperature solid oxide fuel cells using a new $LaGaO_3$ based oxide ion conductor, Journal of the Electrochemical Society 145 (1998) 3177–3183.
[16] L.W. Tai, M. Nasrallah, H. Anderson, D. Sparlin, S. Sehlin, Structure and electrical properties of $La_{1-x}Sr_xCo_{1-y}Fe_yO_3$ I: the system $La_{0.8}Sr_{0.2}Co_{1-y}Fe_yO_3$, Solid State Ionics 76 (1995) 259–271.
[17] R. Shannon, Revised effective ionic radii and systematic studies of interatomic distances in halides and chalcogenides, Acta Crystallographica Section A 32 (1976) 751–767.
[18] K. Zhang, R. Ran, L. Ge, Z. Shao, W. Jin, N. Xu, Systematic investigation on new $SrCo_{1-y}Nb_yO_{3-\delta}$ ceramic membranes with high oxygen semi-permeability, Journal of Membrane Science 323 (2008) 436–443.
[19] Y. Teraoka, H. Zhang, K. Okamoto, N. Yamazoe, Mixed ionic–electronic conductivity of $La_{1-x}Sr_xCo_{1-y}Fe_yO_{3-\delta}$ perovskite-type oxides, Materials Research Bulletin 23 (1988) 51–58.
[20] J. Stevenson, T. Armstrong, R. Carneim, L. Pederson, W. Weber, Electrochemical properties of mixed conducting perovskites $La_{1-x}M_xCo_{1-y}Fe_yO_{3-\delta}$ (M=Sr, Ba, Ca), Journal of the Electrochemical Society 143 (1996) 2722–2729.
[21] J. Zhang, H. Zhao, Y. Li, N. Xu, W. Ding, X. Lu, F. Li, Effects of iron content on the structural evolution, electrical properties and thermochemical stability of $BaCo_{0.9-x}Fe_xNb_{0.1}O_{3-\delta}$ ceramic membrane, International Journal of Hydrogen Energy 35 (2010) 814–820.
[22] R.O. Fuentes, R.T. Baker, Structural, morphological and electrical properties of $Gd_{0.1}Ce_{0.9}O_{1.95}$ prepared by a citrate complexation method, Journal of Power Sources 186 (2009) 268–277.
[23] R.R. Kondakindi, K. Karan, Characterization of Fe- and Mn-doped GDC for low-temperature processing of solid oxide fuel cells, Materials Chemistry and Physics 115 (2009) 728–734.